Specificity in Protein−Protein Recognition: Conserved Im9 Residues Are the Major Determinants of Stability in the Colicin E9 DNase−Im9 Complex[†]

Russell Wallis,[‡,§,||] Kit-Yi Leung,[‡,§] Michael J. Osborne,[⊥,#] Richard James,[‡] Geoffrey R. Moore,[⊥] and Colin Kleanthous*[,‡]

Schools of Biological and Chemical Sciences, University of East Anglia, Norwich NR4 7TJ, U.K.

Received August 1, 1997; Revised Manuscript Received October 29, 1997[⊗]

ABSTRACT: The endonuclease group of E colicins are a family of bacterial toxins whose cytotoxic activity in a producing host is inactivated by a specific immunity protein. The DNase of colicin E9 can be bound and inhibited by both cognate and noncognate immunity proteins, the dissociation constants for which span a range of 12-orders of magnitude. DNase binding specificity of the immunity proteins is governed primarily by helix II, the sequence of which is variable in this family of proteins. Heteronuclear NMR experiments have identified helix III along with helix II as the likely DNase binding site, although other regions of Im9 also showed perturbations on binding the E9 DNase. In the present work, we have used the NMR experiments as a guide for alanine scanning mutagenesis of Im9. Our data show that helices II and III of Im9 are indeed the DNase binding site and in addition quantitate the relative binding energy associated with each helix. We find that the conserved residues of helix III make the largest relative contribution toward E9 DNase binding. In conjunction with previous studies, the data suggest that specificity in the colicin−immunity system is governed by a dual recognition mechanism in which highly stabilizing interactions emanating from the conserved regions of an immunity protein act as the binding site anchor and these are modulated by interactions from neighboring, nonconserved amino acid residues. This modulation is likely to take the form of both favorable and unfavorable interactions, the balance of which define the specificity of the protein−protein interaction. The generality of such a dual recognition mechanism in other systems is also discussed.

Specificity in protein−protein interactions is a poorly understood phenomenon, yet specific recognition of one protein by another underpins many biological processes. We have been addressing questions of specificity in protein−protein recognition in the colicin DNase−immunity protein system. Colicins are a large and varied family of plasmid-encoded bacterial toxins, and immunity proteins are inhibitors that are coproduced to suppress the action of the toxin in the host. Of the many types of bacteriocidal activities that colicins can display we have focused our attention on a class of toxins which are members of the E group colicins and which kill *Escherichia coli* cells through the action of an endonuclease domain (*1*). The toxins initiate cell death by first binding to the vitamin B_{12} receptor of *E. coli* cells followed by translocation across both bacterial membranes. The E group DNase colicins are 61 kDa proteins composed of domains responsible for receptor binding and membrane translocation as well as a C-terminal, nonspecific DNase domain (*2*), which can be overproduced and purified separately from the rest of the toxin (*3*). Within the E group of colicins four DNase-type toxins have been identified, known as colicins E2, E7, E8, and E9, which share a high sequence identity in the regions of the protein implicated in receptor binding and translocation but are only ∼80% identical in their DNase domains (*4*). The DNase activity of each toxin is inhibited by a specific immunity protein, Im2, Im7, Im8, and Im9,[1] respectively, which share ∼50% sequence identity. These are 9.5 kDa proteins which form tight, stoichiometric complexes with their cognate endonucleases (*5*−*7*). The complexes are released from the producing cell into the surrounding environment through the action of a third protein (the lysis protein), and it is as a heterodimeric complex that cell killing begins (*8, 9*).

Recent work from our laboratory has shown that the E colicin DNase−immunity protein system is a rich source of structural and thermodynamic information concerning the specificity of interprotein complexes within families of closely related proteins. The structures for Im9 and Im7, solved by NMR and X-ray crystallography, respectively (*10*−

[†] This work was supported by The Wellcome Trust and the United Kingdom Biotechnology and Biological Sciences Research Council.

* To whom correspondence should be addressed. Tel: +44-1603 593221. Fax: +44-1603 592250. E-mail: c.kleanthous@uea.ac.uk.

[‡] School of Biological Sciences, University of East Anglia.

[§] R.W. and K.-Y.L. contributed equally to this work.

[||] Present address: The Glycobiology Institute, Department of Biochemistry, University of Oxford, South Parks Road, Oxford OX1 3QU, U.K.

[⊥] School of Chemical Sciences, University of East Anglia.

[#] Present address: The Scripps Research Institute, 10666 North Torrey Pines Road, La Jolla, CA 92037.

[⊗] Abstract published in *Advance ACS Abstracts,* December 15, 1997.

[1] Abbreviations: ColE9, colicin E9; E9 DNase, the isolated 15 kDa endonuclease domain of ColE9; Im9, immunity protein specific for ColE9; k_1, association rate constant; k_{off}, the overall dissociation rate constant; K_d, equilibrium dissociation constant; Gdn·HCl, guanidine hydrochloride; HSQC, heteronuclear single-quantum coherence.

S0006-2960(97)01884-9 CCC: $15.00
Published on Web 01/13/1998

12), are similar and best described as distorted, antiparallel four-helix proteins. Im9 binds to its cognate endonuclease, in the form of the whole toxin or the isolated 15 kDa E9 DNase domain, with an equilibrium dissociation constant (K_d) of 10^{-16} M in buffers of low ionic strength, which is one of the tightest protein complexes yet reported in the literature (*13*). The two proteins associate at the rate of diffusion to form an encounter complex which undergoes a slow conformational change to yield the final stable complex. The noncognate immunity proteins will also bind and inhibit the activity of the E9 DNase but with much weaker affinities, 10^{-4} M for Im7, 10^{-6} M for Im8, and 10^{-8} M for Im2. The complexes formed with the Im2 and Im8 proteins also go through a two-state association mechanism with rate constants almost identical to those of Im9, implying that the same conformational change is triggered by cognate and noncognate immunity protein binding alike (*14*). The noncognate complexes, however, dissociate $>10^6$-fold faster than Im9. The resulting binding affinities for this family of homologous proteins for the E9 DNase span 12 orders of magnitude which essentially matches the entire range of known thermodynamic stabilities for protein complexes described in the literature (*14*).

Homologue scanning mutagenesis has shown that the specificity of an immunity protein for its target endonuclease derives almost entirely from helix II, which is variable in sequence in this family of proteins (*15*). Substituting this helix from Im9 into the Im2 framework switches the biological specificity of Im2 so that it now becomes specific for ColE9. The resulting chimeric immunity protein binds almost as tightly to the E9 DNase as wild-type Im9. By including buried sequences from helix I which interact with helix II, full E9 DNase binding is obtained, implying that helix packing also plays a role in specificity, presumably by controlling the precise orientation of residues from helix II.

While it is clear which regions of an immunity protein govern its specificity, what is still unresolved is how they inactivate a colicin endonuclease and what mechanism of recognition is adopted which enables proteins sharing more than 50% sequence identity to bind to the E9 DNase with dissociation constants that span the millimolar to femtomolar affinity range. A clue to this mechanism has come from heteronuclear NMR experiments in which the E9 DNase binding site on the Im9 protein has been delineated (*16*). The amide resonances of ^{15}N-labeled Im9 in complex with the 15 kDa E9 DNase domain have been assigned and chemical shift perturbations categorized using ^{1}H−^{15}N HSQC experiments. Helix II, the specificity helix, is strongly perturbed along with residues from helix III, which is conserved in the immunity protein family. In the present work, we have conducted an alanine scan across this putative E9 DNase binding surface of Im9 and quantified the relative binding energy of amino acid side chains. The alanine scanning data confirm that helices II and III are the DNase binding site and reveal for the first time the relative contributions to binding of conserved and nonconserved regions of the immunity protein. We suggest a mechanism of DNase selectivity for the immunity proteins based on these data and discuss the relevance of this mechanism in terms of other protein−protein recognition systems.

MATERIALS AND METHODS

Bacterial Strains and Media. *E. coli* strains JM105 (*supE*, *endA*, *sbcB*15, *hsdR*4, *rpsL*, *thi*, Δ(*lac-proAB*), F′ [*traD36*, *proAB*$^+$, *lacI*^{q}, l*acZ*ΔM15]) and JM83 hsdR, a restriction-deficient derivative of *E. coli* JM83 (*Ara*$^+$, *Lac*$^+$, *Pro*, *thi*, *rpsL*, ø80Δ*lacZ*M15), were used as the host strain for the plasmids. Cultures were grown in Luria−Bertani (LB) broth or on plates of LB agar, supplemented where necessary with ampicillin (100 μg/mL).

Site-Directed Mutagenesis, Protein Purifications, and Protein Determinations. Purification of the DNase domain of colicin E9, the Im9 protein, and tritiated Im9 ([^{3}H]Im9) have all been described previously (*3*, *7*, *13*). Site-directed mutagenesis of the *imm*9 gene was carried out as described by Osborne et al. (*16*). The resulting immunity gene was cloned into the expression vectors pTrc99A or pKK233-2 (Pharmacia) and introduced into the the host *E. coli* strain JM83 by transformation. In each case, the directed mutation and the entire immunity gene sequence were verified by double-stranded DNA sequencing using an ALF sequencer (Pharmacia) and the reagents and protocols supplied by Pharmacia. Expression was induced by the addition of 1 mM isopropyl β-D-thiogalactoside at an optical density at 550 nm of between 0.6 and 0.8 and the protein purified as described previously for the Im9 protein (*7*).

Protein concentrations were determined by amino acid analysis and from the absorbance at 280 nm. The molar absorption coefficients determined for the proteins are E9 DNase, 17 550 M^{-1} cm^{-1}, and Im9, 11 400 M^{-1} cm^{-1} (*13*).

Electrospray Mass Spectrometry. The mass of each purified protein was confirmed by eletrospray mass spectrometry as described previously (*17*).

Association Kinetics. Stopped-flow kinetic measurements were made using an Applied Photophysics biosequential stopped-flow spectrofluorometer (slit widths = 5 nm) using an excitation wavelength of 280 nm and monitoring the fluorescence emission above 320 nm. All reactions were performed in 50 mM Mops buffer, pH 7.0, containing 200 mM NaCl and 1 mM dithiothretol (DTT), at 25 °C, essentially as described by Wallis et al. (*13*). Association between the E9 DNase and Im9 was monitored under pseudo-first-order conditions using a 4−20-fold excess of immunity protein over E9 DNase (0.35 μM). The resulting biphasic fluorescence traces were fitted to a double exponential equation.

Dissociation Kinetics. Dissociation rate constants were determined by radioactive subunit exchange using strategies similar to those described previously (*13*−*15*). For Im9 Asp51Ala, where the dissociation rate constant is less than the limiting value of the radioactive method (3.9×10^{-3} s^{-1}; $t_{1/2} < 3$ min) dissociation was monitored by stopped-flow fluorescence. The E9 DNase (5 μM) was premixed with a slight excess of Im9 Asp51Ala (6 μM) and chased with an equal volume of a 10-fold excess of Im9 Tyr54Ala (60 μM). The data were fitted to a first-order rate equation.

Data Analysis. A two-step reaction model has been proposed by Wallis et al. (*13*) for the interaction of the E9 DNase with Im9 (eq 1), where nuclease (N) and immunity protein (I) form an encounter complex (NI*) in a rapid binding step, which then undergoes a slow isomerization to the final bound state (NI).

$$N + I \underset{k_{-1}}{\overset{k_1}{\rightleftharpoons}} NI^* \underset{k_{-2}}{\overset{k_2}{\rightleftharpoons}} NI \quad (1)$$

In this case, the equilibrium dissociation constant is given by the expression:

$$K_d = (k_{-1}/k_1)/[1 + (k_2/k_{-2})] \quad (2)$$

For the E9 DNase−Im9 complex, the rate of formation of the encounter complex is rate determining for the forward reaction and hence $K_d = k_{off}/k_1$, where k_{off} is the overall dissociation rate constant measured by subunit exchange kinetics and k_1 is the bimolecular association rate constant measured by stopped-flow fluorescence (*13*). Values of $\Delta\Delta G_{binding}$ were calculated as $+RT \ln[K_d(\text{mutant})/K_d(\text{wild type})]$, where R is the gas constant and T is the absolute temperature.

Immunity Protein Denaturation and Stability. Fluorescence spectroscopy was used to monitor the denaturation of immunity proteins and to determine their relative stabilities. All experiments were conducted with a Shimadzu RF5000 spectrofluorometer, thermostated at 25 °C in filtered 50 mM potassium phosphate buffer, pH 7.0, using an excitation wavelength of 295 nm to ensure only tryptophan excitation. The excitation and emission bandwidths were 5 nm, and 3 mL quartz cuvettes were used throughout. Each immunity protein (generally 1−2 μM) was equilibrated in buffer containing guanidine hydrochloride (0−3 M, for a minimum of 2 h at 25 °C), and the fluorescence emission was observed at 354 nm, with the exception of Im9 Pro47Ala where fluorescence measurements were recorded at 370 nm, which was the wavelength showing the greatest difference in fluorescence intensity between the folded and unfolded states.

The relative immunity protein stabilities were determined using strategies similar to those described by Kellis et al. (*18*). For small differences where denaturation curves overlap the relative stability was determined at a single concentration of Gdn·HCl near the midpoint of the denaturation curve of wild-type Im9 (1.6 M Gdn·HCl) by

$$\Delta\Delta G_{stability} = RT \ln[(\text{folded/unfolded})_{\text{wild type}}/(\text{folded/unfolded})_{\text{mutant}}] \quad (3)$$

For large differences in stabilities (His46Ala, Pro47Ala, Leu52Ala, Ile53Ala, Tyr54Ala, Leu36Ala, Val37Ala, Ser63Ala, and Val68Ala) where the denaturation transitions do not overlap, the relative stability was determined by extrapolating the free energy of unfolding at each individual concentration of Gdn·HCl to an intermediate concentration for the wild-type and mutant curves. This assumes linearity in the dependence of ΔG on Gdn·HCl only over a small range beyond the experimental data. The intermediate Gdn·HCl concentrations used were 1.2 M for His46Ala and 1 M for Leu33Ala, Leu36Ala, Val37Ala, Pro47Ala, Leu52Ala, Ile53Ala, Tyr54Ala, Ser63Ala, and Val68Ala.

Accessibility Determination of Side Chains. The accessible surface areas of the mutated amino acid side chains of Im9 were obtained from calculations based on its NMR structure using the program SURFACE from the Collaborative Computational Project No. 4 program suite (Daresbury laboratory, Warrington, Cheshire, U.K.). These were expressed as the percent exposure of the side chain to the solvent relative to the accessible surface of the same residue in a tripeptide model of Gly-X-Gly (*19*).

RESULTS

Candidates for Alanine Mutagenesis. A putative E9 DNase binding site has been identified through heteronuclear NMR experiments on ^{15}N-labeled Im9 bound to the unlabeled E9 DNase domain (*16*). The NMR data were obtained from 2D ^{1}H−^{15}N HSQC spectra which allowed the complexation-induced perturbations of the Im9 amide resonances to be quantified. More than 60 of the 86 amide resonances were perturbed to some degree on binding the DNase, and these fell into three general categories: the "large" chemical shift perturbation category consisted of residues 27−29, 34, 35, 38, 49, 50, and 53−55, the "intermediate" category comprised residues 23, 33, 36, 41−44, 46, 48, 52, 60, 63, 68, and 69, and the small category contained the remaining residues (Figure 1; see figure legend for details of the NMR analysis). Twenty-six residues in total were identified within the large and intermediate categories, the majority of which (20 from the 26) fell between residues 27−55 and include helix II, helix III, the turn that connects them, and the loop connecting helix I and helix II (Figure 1). Five residues (Cys23, Glu31, Val34, Glu42, and Tyr54), which represented the three chemical shift perturbation categories, were mutated to alanine and their dissociation rate constants from complexes with the E9 DNase determined. The observed changes in off-rates showed general agreement with the chemical shift categorization of these residues, supporting the way in which the E9 DNase binding site had been assigned (*16*).

The alanine scan presented in this paper is focused around residues whose amides showed large and intermediate changes in chemical shift on binding the E9 DNase since these seemed the most likely to encompass the DNase binding site. We have continued with the characterization of the five original mutants described above and have determined their association rate constants and hence the equilibrium dissociation constants for the mutant Im9−E9 DNase complexes. A further 29 alanine mutants have been constructed representing most of the residues highlighted by NMR but also including ten residues (24, 26, 30−32, 37, 45, 47, 51, and 56) which fell below the chemical shift cutoffs used to define the DNase binding site. This latter group was chosen because their location in Im9 suggested a possible role in binding.

Im9 alanine mutants were overproduced and purified as described in the Materials and Methods section and the masses of purified proteins confirmed by electrospray mass spectrometry. In each case, the masses of the mutant proteins corresponded to the predicted mass to within 1 Da (data not shown). Stability and kinetic measurements were carried out twice on each preparation of mutant protein. The equilibrium dissociation constants for the mutants were determined from the individual association and dissociation rate constants as described in the Materials and Methods section.

Association Kinetics. Stopped-flow fluorescence was used to determine the association rate constant, k_1, for each of the 34 alanine mutants. Association between the E9 DNase and Im9 is essentially diffusion controlled in buffer of low

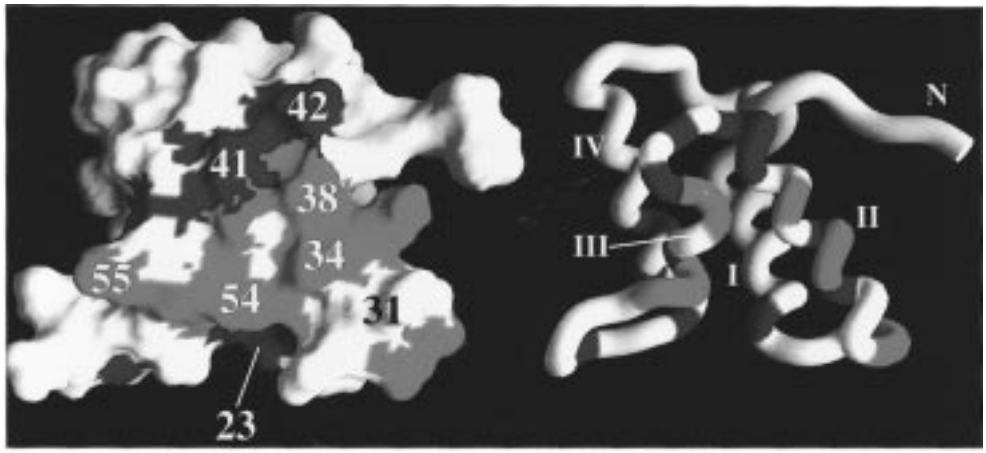

FIGURE 1: Structure of Im9 showing the amide resonances which are perturbed on binding the E9 DNase in $^1H-^{15}N$ HSQC experiments. The figure was adapted from Osborne et al. (*16*). Color code: red, large chemical shift changes (1−3 and/or 0.2−0.6 ppm in the ^{15}N and ^1H dimensions, respectively); blue, intermediate chemical shift changes (0.2−1 and 0.04−0.2 ppm in the ^{15}N and ^1H dimensions, respectively); white, residues showing either no changes in chemical shift or changes <0.2 ppm in the ^{15}N dimension and <0.04 ppm in the ^1H dimension.

ionic strength (*13*). Therefore, in order to reduce the magnitude of the association rate to enable accurate determination of k_1 under pseudo-first-order conditions, 200 mM NaCl was included in all the experiments. For each of the alanine mutants, a biphasic association profile was observed on binding the E9 DNase, similar to that determined for wild-type Im9, in which an initial fluorescence enhancement, due to the bimolecular collision of the two proteins, is followed by a fluorescence quench, due to a conformational change in the DNase (*13*, *14*). Under the conditions used in the current experiments (pH 7.0, 200 mM NaCl, and 25 °C) k_1 for Im9 binding to the E9 DNase is $\sim 1 \times 10^8$ M^{-1} s^{-1} and the rate of the conformational change is 4−5 s^{-1}. Values of k_1 for each of the mutant Im9−E9 DNase complexes are listed in Table 1 and depicted in Figure 2A. The association rate constants vary little (<3-fold) for most of the alanine mutants, the largest differences observed for mutations of acidic residues Asp51Ala and Glu41Ala where k_1 is reduced by 6- and 4-fold, respectively. The effects of these substitutions are consistent with electrostatic steering playing an important role in the bimolecular collision, in agreement with previous studies of the E9 DNase−Im9 complex (*13*). A further point relating to the magnitude of these effects is that the electrostatic contribution to association will be diminished due to the presence of 200 mM NaCl in the reaction buffer, implying that these differences would be even larger in the absence of salt. For each of the alanine mutants, the rate constant of the fluorescence quench step was similar to that for the wild-type immunity protein, showing that the conformational change that follows the formation of the encounter complex is not compromised by any of the mutants.

Dissociation Kinetics and Binding Energies. The dissociation rate constant (k_{off}) for most of the mutant complexes was determined by radioactive exchange kinetics in which the unlabeled mutant complex was chased with radiolabeled Im9 (*13*−*16*). In each case, the exchange process was followed to at least 50%, and the data were fitted using first-order kinetics. This technique for determining k_{off} can only be used for complexes with slow dissociation rates ($k_{off} < 4 \times 10^{-3}$ s^{-1}). For the Asp51Ala complex, the off-rate is faster than this, and so a stopped-flow fluorescence experiment was devised to determine this rate constant. This experiment

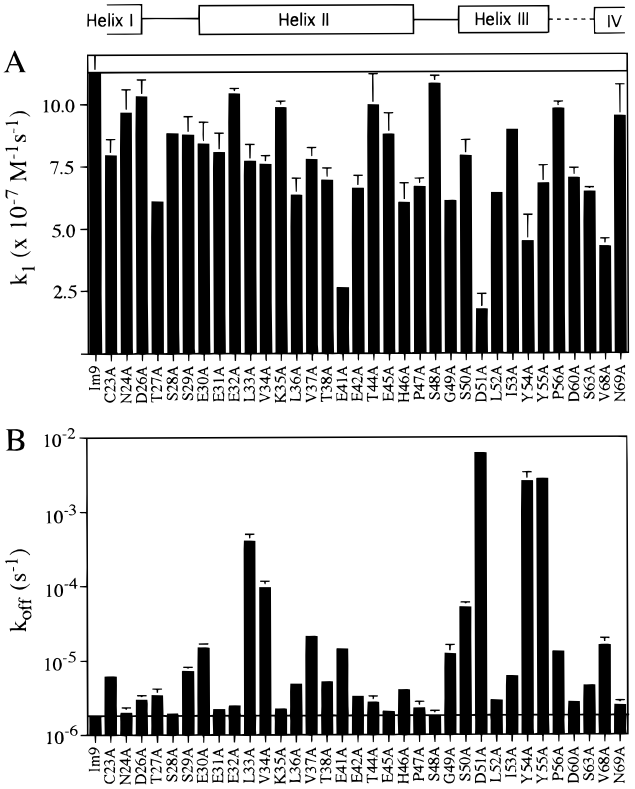

FIGURE 2: Association and dissociation rate constants of alanine mutations. Panel A shows the effect of Im9 alanine substitutions on the rate of association (k_1) of the E9 DNase with Im9 (see Materials and Methods section for details). The horizontal line represents k_1 for the wild-type Im9−E9 DNase complex. Panel B shows the effect of Im9 alanine substitutions on the dissociation rate constant (k_{off}) of E9 DNase−Im9 complexes. With the exception of the Asp51Ala mutant, rate constants were determined by radioactive subunit exchange. The dissociation rate constants were calculated as described previously (*13*, *14*) and are summarized in the Materials and Methods section. The horizontal line represents k_{off} for the wild-type Im9−E9 DNase complex. In both panels, the error bars represent the standard errors from duplicate experiments. The secondary structure shown above the figure represents the main structural elements of Im9 which were targetted for mutagenesis. The choice of residues which were mutated within these structural elements is explained in the text.

relies on the observation that binding of Im9 Tyr54Ala to the E9 DNase results in a significantly lower fluorescence

Table 1: Kinetic and Thermodynamic Parameters for the Im9 Alanine Mutants[a]

	$k_1 \times 10^{-7}$ (M^{-1} s^{-1})[b]	k_{off} (s^{-1})[c]	K_d (M)[d]	$\Delta\Delta G_{binding}$ (kcal/mol)[e]	$\Delta\Delta G_{stability}$ (kcal/mol)[f]	accessibility (%)[g]
Im9	11.3 (±0.8)	1.83 (±0.09) × 10^{-6}	1.62 × 10^{-14}			
C23A	7.9 (±0.7)	6.09 (±0.69) × 10^{-6}	7.68 × 10^{-14}	0.92 (±0.04)	0.98 (±0.21)	59.8
N24A	9.6 (±1.0)	1.98 (±0.36) × 10^{-6}	2.05 × 10^{-14}	0.14 (±0.10)	0.47 (±0.02)	39.3
D26A	10.3 (±0.7)	2.95 (±0.46) × 10^{-6}	2.86 × 10^{-14}	0.34 (±0.06)	−0.08 (±0.01)	44
T27A	6.1 (±0.1)	3.37 (±0.79) × 10^{-6}	5.54 × 10^{-14}	0.73 (±0.08)	0.56 (±0.04)	1.7
S28A	8.8 (±0.1)	1.91 (±0.03) × 10^{-6}	2.17 × 10^{-14}	0.17 (±0.06)	−0.16 (±0.00)	68.3
S29A	8.8 (±0.8)	7.13 (±1.10) × 10^{-6}	8.14 × 10^{-14}	0.96 (±0.07)	0.89 (±0.07)	66.6
E30A	8.4 (±0.9)	1.48 (±0.20) × 10^{-5}	1.77 × 10^{-13}	1.41 (±0.07)	0.09 (±0.02)	89.6
E31A	8.1 (±0.8)	2.19 (±0.14) × 10^{-6}	2.72 × 10^{-14}	0.31 (±0.02)	−0.24 (±0.07)	80.5
E32A	10.4 (±0.3)	2.44 (±0.25) × 10^{-6}	2.35 × 10^{-14}	0.22 (±0)	0.43 (±0.25)	50.2
L33A	7.7 (±0.7)	4.00 (±1.00) × 10^{-4}	5.20 × 10^{-12}	3.42 (±0.13)	1.61 (±0.54)	9.9
V34A	7.6 (±0.4)	9.54 (±2.10) × 10^{-5}	1.26 × 10^{-12}	2.58 (±0.09)	0.28 (±0.09)	55.9
K35A	9.8 (±0.3)	2.20 (±0.20) × 10^{-6}	2.24 × 10^{-14}	0.19 (±0)	0.35 (±0.03)	80.2
L36A	6.3 (±0.7)	4.75 (±0.48) × 10^{-6}	7.49 × 10^{-14}	0.91 (±0.05)	1.73 (±0.16)	20
V37A	7.8 (±0.5)	2.09 (±0.27) × 10^{-5}	2.69 × 10^{-13}	1.66 (±0.04)	1.90 (±0.12)	2.5
T38A	6.9 (±0.5)	5.13 (±0.38) × 10^{-6}	7.40 × 10^{-14}	0.90 (±0.01)	0.22 (±0.01)	63.9
E41A	2.6 (±0.1)	1.42 (±0.89) × 10^{-5}	5.46 × 10^{-13}	2.08 (±0.02)	0.08 (±0.19)	43.4
E42A	6.6 (±0.5)	3.25 (±0.15) × 10^{-6}	4.92 × 10^{-14}	0.66 (±0)	0.33 (±0.04)	79.7
T44A	9.9 (±1.3)	2.70 (±0.61) × 10^{-6}	2.71 × 10^{-14}	0.30 (±0.14)	0.21 (±0.03)	0
E45A	8.8 (±0.9)	2.04 (±0.18) × 10^{-6}	2.32 × 10^{-14}	0.21 (±0.04)	0.82 (±0.06)	61.9
H46A	6.0 (±0.8)	3.98 (±0.28) × 10^{-6}	6.60 × 10^{-14}	0.83 (±0.05)	2.68 (±0.27)	9
P47A	6.7 (±0.3)	2.26 (±0.52) × 10^{-6}	3.39 × 10^{-14}	0.44 (±0.10)	2.89 (±0.17)	49.8
S48A	10.8 (±0.3)	1.77 (±0.32) × 10^{-6}	1.64 × 10^{-14}	0.01 (±0.05)	−0.10 (±0.06)	15.9
G49A	6.1 (±0.1)	1.22 (±0.40) × 10^{-5}	1.99 × 10^{-13}	1.49 (±0.14)	0.83 (±0.06)	0
S50A	7.9 (±0.7)	5.14 (±0.84) × 10^{-5}	6.51 × 10^{-13}	2.19 (±0.07)	0.08 (±0.02)	40.7
D51A	1.7 (±0.6)	6.11 (±0.16) × 10^{-3}	3.53 × 10^{-10}	5.92 (±0.17)	0.50 (±0.02)	23.4
L52A	6.4 (±0.1)	2.87 (±0.13) × 10^{-6}	4.47 × 10^{-14}	0.60 (±0.03)	3.36 (±0.37)	10.8
I53A	8.9 (±0.1)	6.06 (±0.70) × 10^{-6}	6.78 × 10^{-14}	0.85 (±0)	3.51 (±0.23)	4.1
Y54A	4.5 (±1.1)	2.55 (±0.85) × 10^{-3}	5.69 × 10^{-11}	4.83 (±0.28)	2.90 (±0.25)	44.8
Y55A	6.9 (±0.7)	2.75 (±0.15) × 10^{-3}	4.06 × 10^{-11}	4.63 (±0.03)	0.18 (±0.17)	71.1
P56A	9.8 (±0.3)	1.30 (±0.09) × 10^{-5}	1.32 × 10^{-13}	1.24 (±0.02)	0.60 (±0.02)	33.4
D60A	7.0 (±0.4)	2.69 (±0.29) × 10^{-6}	3.84 × 10^{-14}	0.51 (±0.03)	−0.10 (±0.10)	53.4
S63A	6.5 (±0.2)	4.54 (±0.42) × 10^{-6}	7.04 × 10^{-14}	0.87 (±0)	1.80 (±0.06)	48.8
V68A	4.3 (±0.3)	1.59 (±0.39) × 10^{-5}	3.72 × 10^{-13}	1.86 (±0.12)	2.10 (±0.03)	0.5
N69A	9.5 (±1.3)	2.46 (±0.40) × 10^{-6}	2.59 × 10^{-14}	0.28 (±0.11)	−0.42 (±0.31)	61.2

[a] Standard errors from duplicate observations are shown in parentheses. [b] Im9−E9 DNase association rate constants determined by stopped-flow fluorescence. [c] Im9−E9 DNase dissociation rate constants determined by radioactive exchange kinetics, except for Asp51Ala which was determined by a stopped-flow experiment as described in the text. [d] Im9−E9 DNase dissociation constants calculated according to the equation k_{off}/k_1 (*13*). [e] $\Delta\Delta G_{binding}$ was calculated with respect to wild-type Im9 binding the E9 DNase domain. [f] $\Delta\Delta G_{stability}$ was determined from guanidine hydrochloride denaturation of each protein and calculated relative to wild-type Im9. [g] Amino acid side-chain accessibility is shown as a percentage relative to the accessibility of that residue in a Gly-X-Gly sequence (*19*).

enhancement compared to wild-type Im9 (and Im9 Asp51Ala) (data not shown). A complex of Im9 Asp51Ala and E9 DNase was therefore chased with Im9 Tyr54Ala. The subsequent fluorescence decay was fitted to a first-order rate equation and provides a direct measure of the off-rate for this complex (data not shown). From the relative fluorescence intensities of each complex, the overall fluorescence change was found to correspond closely to the estimated value assuming complete exchange. Similar fluorescence chase experiments have been used to determine off-rates for noncognate E9 DNase−Im9 protein complexes (*14*). Values of k_{off} for each of the mutant Im9−E9 DNase complexes are listed in Table 1 and shown in Figure 2B. The dissociation rate constant of the native complex under the conditions used is $\sim 2 \times 10^{-6}$ s^{-1}.

Values of $\Delta\Delta G_{binding}$ relative to wild-type Im9 were calculated from the dissociation constants (where $K_d = k_{off}/k_1$) for all the alanine mutants as described in the Materials and Methods section, and the data are presented in Table 1. The alanine substitutions range from those that have little or no effect on the relative binding energy (e.g., Asp26Ala or Glu32Ala) to those that have intermediate effects in the range 1−3 kcal/mol (e.g., Glu41Ala and Ser50Ala) and those that have substantial effects on binding of the order of 3−6 kcal/mol (e.g., Asp51Ala, Tyr54Ala, and Val34Ala). The binding energies are depicted on the structure of free Im9 in Figure 5b,e.

The stability of the E9 DNase−Im9 complex is governed by the rate of complex dissociation, and so alanine mutations which affect binding do so by increasing k_{off} (Table 1 and Figure 2B). This phenomenon has been well documented in other systems such as growth hormone binding to its cognate receptor (*20*) and barnase binding to barstar (*21*). The dependence of complex affinity on the rate of dissociation has been discussed in the literature (for example, *22*) and reflects the large number of interactions that have to be broken in order that the complex can dissociate. Consequently, there is a large activation barrier for dissociation, estimated for the E9 DNase−Im9 complex from Arrhenius plots as 26 kcal/mol (*13*). By contrast, the activation barrier for association between the E9 DNase and Im9 is very low (~4 kcal/mol), reflecting the fact that it is a diffusion-controlled process.

Stabilities of the Im9 Alanine Mutants. The side chains for some of the residues of Im9 whose amide chemical shift resonances were perturbed in the original NMR experiments are partially or completely buried in the unbound protein (*11, 16*). However, since the structure of bound Im9 is not

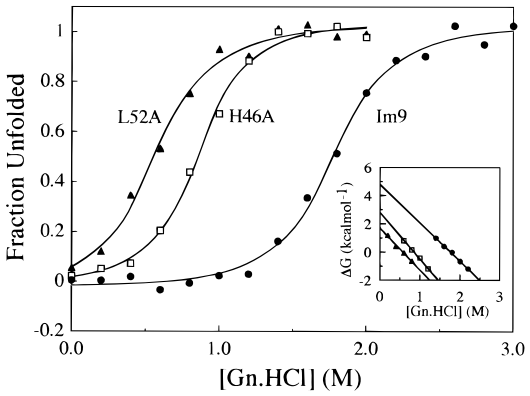

FIGURE 3: Denaturation of Im9 and the His46Ala and Leu52Ala mutants by guanidine hydrochloride monitored by fluorescence spectroscopy. The denaturation of wild-type and mutant immunity proteins was monitored by tryptophan fluorescence emission at 354 nm and plotted as a function of the total change in emission intensity. (Inset) ΔG values were calculated at points across the denaturation transition as described in the Materials and Methods section. The stabilities relative to wild-type Im9 ($\Delta\Delta G_{stability}$) were determined at intermediate guanidine hydrochloride concentrations of 1 and 1.2 M for Leu52Ala and His46Ala, respectively.

known, the direct involvement of such residues in binding the E9 DNase remains a possibility. Hence these residues were also substituted for alanine. As a result, many of the alanine mutations might be expected to affect the conformational stability of Im9, and so it was of interest to determine the stabilities of all the alanine mutants. Another reason for investigating their stabilities stems from our recent observation that mutations which affect immunity specificity often affect the stability of the protein as well (*15*).

The conformational stability ($\Delta\Delta G_{stability}$) for each alanine mutant relative to wild-type Im9 was determined using guanidine hydrochloride (Gdn·HCl) induced denaturation and tryptophan emission fluorescence spectroscopy. The fluorescence emission maximum of Im9 is 334 nm and shifts to 354 nm on denaturation. Coincident with denaturation is a 5-fold increase in fluorescence, indicating that the emission from the single conserved tryptophan (Trp74) in Im9 is highly quenched in the native protein. The native and denatured fluorescence spectra of the majority of the Im9 alanine mutant proteins were similar to those of Im9. However, for some of the more destabilized mutants, such as His46Ala and Pro47Ala, the fluorescence intensity of the native proteins was increased relative to Im9 and the λ_{max} was shifted to the red, indicating greater exposure of the tryptophan residue. Both of these residues lie close to Trp74; indeed, the imidazole of His46 forms a stacking interaction with the indole ring, which is consistent with their effects on fluorescence and the stability of the protein.

Im9 displays a single, cooperative and reversible denaturation transition from which the ΔG_{H_2O} was determined, according to the method of Pace (*23*), to be −4.8 kcal/mol. The relative stabilities of each of the alanine mutants were determined as described in the Materials and Methods section. The denaturation curve of Im9 in Gdn·HCl, together with those of two of the most destabilized alanine mutants, Im9 Leu52Ala and His46Ala, is shown in Figure 3.

$\Delta\Delta G_{stability}$ values for all the alanine mutants are listed in Table 1. In general, the mutation of buried residues in a protein is expected to have a greater effect on stability than

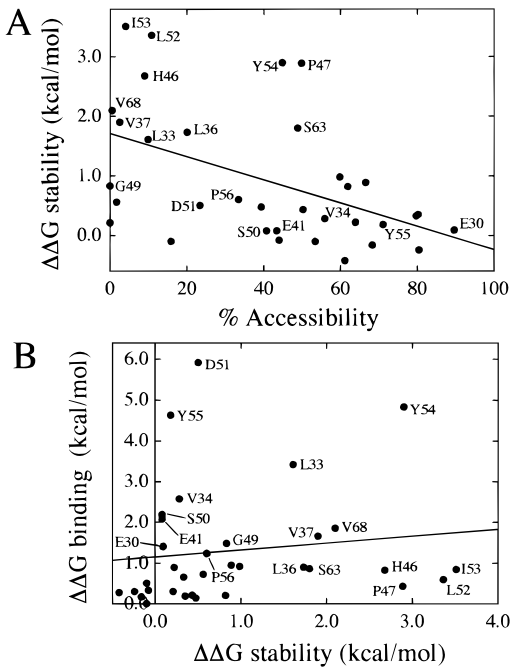

FIGURE 4: Effect of alanine substitutions on Im9 stability and E9 DNase binding affinity. (A) Changes in thermodynamic stability ($\Delta\Delta G_{stability}$) of Im9 alanine mutants plotted against the degree of accessibility of each side chain in Im9, the structure of which has been determined by NMR (*11*). The data are also listed in Table 1. Side-chain accessibilities were calculated as described in the Materials and Methods section. The fitted line indicates a least squares fit to the data and serves to emphasize residues which severely destabilize the protein. (B) Changes in E9 DNase binding affinity ($\Delta\Delta G_{binding}$) plotted against changes in thermodynamic stability ($\Delta\Delta G_{stability}$) of the Im9 alanine mutants. The fitted line indicates a least squares fit to the data. Those residues falling on or above the line are likely to delineate the E9 DNase binding epitope (see text for details).

the mutation of surface-exposed residues. To test this in the case of Im9, changes in protein stability of the alanine mutants were compared with the degree of exposure of each side chain (Figure 4A), where surface accessibility was calculated relative to the exposure of that side chain in the tripeptide Gly-X-Gly (*19*). The stability and accessibility data in Figure 4A show a reasonable correlation; as accessibility of the side chain decreases, the changes in stability increase. As might be expected, buried hydrophobic residues are highly destabilizing when mutated to alanine ($\Delta\Delta G_{stability}$ > 1 kcal/mol). Two notable exceptions, however, are Pro47 and Tyr54, which have significant portions of their side chains exposed to solvent but are very destabilizing when mutated to alanine ($\Delta\Delta G_{stability}$ = 2.9 kcal/mol), reflecting their important structural roles. Pro47 is part of the turn between helices II and III which helps sculpt the interactions around Trp74, and the side chain of Tyr54 sits in a pocket made up of Ile53 and Ser50 of helix III and Val37 of helix II. The crystal structure of Im7 shows the equivalent tyrosine residue forming a hydrogen bond with the base of helix I, thereby tethering the N- and C-terminal halves of the protein (*12*). This interaction is not apparent in the current solution structure of Im9, but this may be a consequence of insufficient distance restraints.

Correlation between the Alanine Scan and NMR Data: Identification of the DNase Binding Site on Im9. Comparisons of binding surfaces determined from NMR experiments

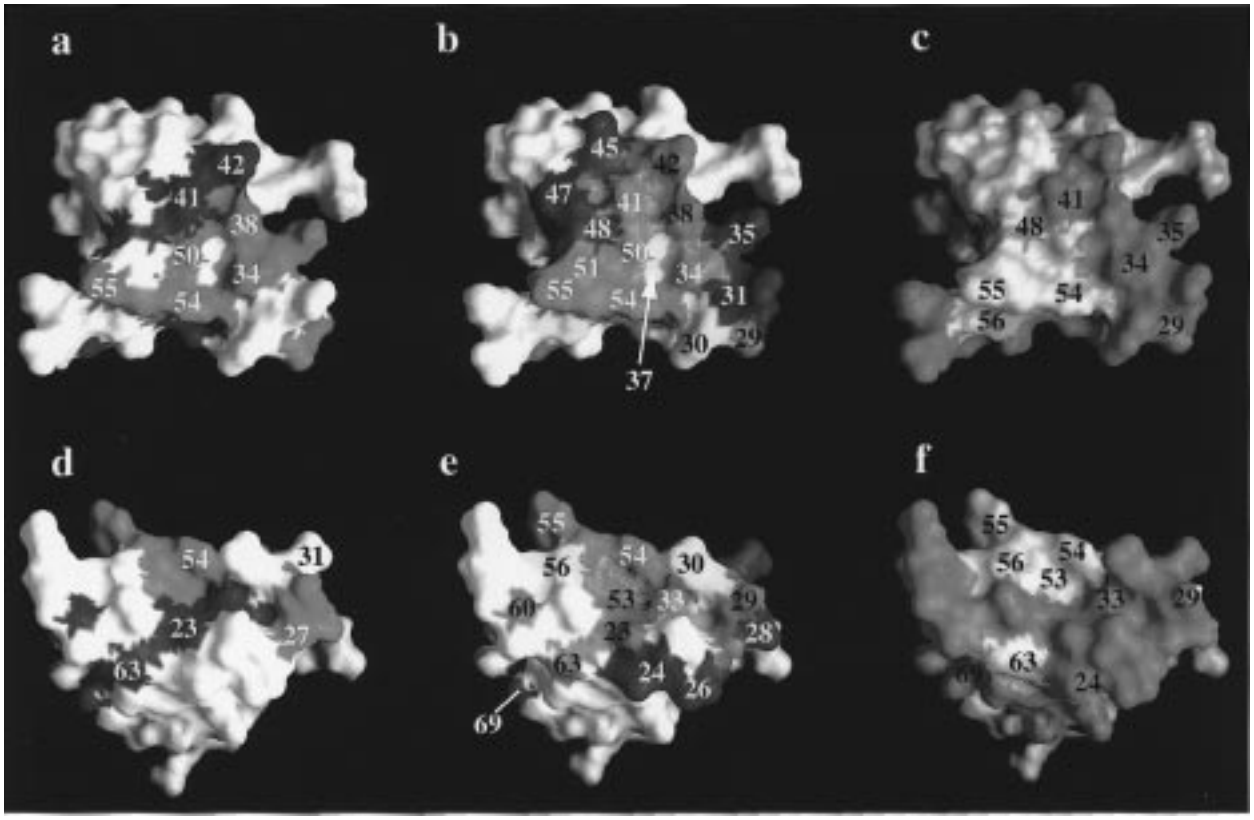

FIGURE 5: Comparison of binding energy data mapped onto surface representations of Im9 with previous NMR data and how they relate to sequence conservation in the immunity protein family. Paired representations of the Im9 structure depicting the amides that are perturbed in HSQC experiments on binding the E9 DNase (a and d), the $\Delta\Delta G_{binding}$ map derived from the alanine scan (b and e), and the sequence conservation in the immunity protein family (c and f) are shown. Parts a−c all show the same surface of Im9 in which helix II (residues 30−46) is on the right, and this is joined by a β-turn (residues 47−49) to helix III (residues 50−55) on the left. Parts d−f show the underside of the protein in which the molecule has been rotated by 90°. Color coding for the different representations: HSQC amide perturbation analysis (a and d) (as described in Figure 1); red, large chemical shift changes on binding the E9 DNase; blue, intermediate chemical shift changes on binding the E9 DNase. Binding energy map of the DNase recognition surface (b and e); red, 4−6 kcal/mol; magenta, 2−4 kcal/mol; yellow, 1−2 kcal/mol; green, 0.5−1 kcal/mol; blue, <0.5 kcal/mol; white, residues not tested. Sequence conservation (c and f); green, residues that are variable throughout the immunity protein family; pink, residues that are completely conserved in the immunity protein family.

with crystal structures of protein complexes have shown that perturbed NMR resonances give a good estimate of the binding surface but that shifts outside the interaction site are also observed (*24*, *25*). The expectation then is that not all of the $^1H-^{15}N$ amide perturbations which occur in Im9 originate from residues within the DNase binding site. The NMR perturbation data of Osborne et al. (*16*), depicted on the structure of free Im9 in Figure 5, suggest that the main area of DNase recognition is the surface made up of residues displayed from helix II and helix III (Figure 5a) but that significant amide shifts are also observed in other regions (Figure 1), most notably on the underside of this surface (Figure 5d). Using these data as a guide, it should be possible to distinguish energetically important residues from unimportant sites by alanine mutagenesis.

Alanine mutants of Im9 might be expected to display one of four effects; (1) changes in E9 DNase binding, (2) changes in Im9 stability, (3) changes to binding and stability, or (4) no effect. A plot of $\Delta\Delta G_{binding}$ against $\Delta\Delta G_{stability}$ (Figure 4B) shows that each of these categories of mutants can be identified. Residues lying close to the *y*-axis (>1 kcal/mol) are those which affect binding, with minimal change in protein stability. Conversely, residues lying close to the *x*-axis (>1 kcal/mol) are those which disrupt protein stability significantly but not DNase binding. Residues toward the center of the plot perturb both binding and stability while those clustered around the origin (<1 kcal/mol on each axis) have little effect on either property.

The least squares fit of $\Delta\Delta G_{binding}$ against $\Delta\Delta G_{stability}$ (Figure 4B) intersects the *y*-axis at ~1 kcal/mol, and we have used this as the basis for identifying the E9 DNase binding site. A $\Delta\Delta G_{binding}$ of 1 kcal/mol is equivalent to an increase in the dissociation rate constant for the complex of 5.4-fold (assuming the association rate constant remains unaffected), which seems a reasonable cutoff considering the largest increase in k_{off} that we measured (for the Asp51Ala mutation) was >3000-fold ($\Delta\Delta G_{binding} = 5.9$ kcal/mol). Following on from this analysis of $\Delta\Delta G_{binding}$, two distinct groups of mutants emerge which help delineate the functional epitope on Im9: (1) those which fall below the fitted line, indicating a relatively small effect on binding ($\Delta\Delta G_{binding} = 0-1$ kcal/mol), and (2) those which coincide with or lie above the fitted line, indicating a significant effect on binding ($\Delta\Delta G_{binding} = 1-6$ kcal/mol). Using these criteria a total of 12 residues can be identified which perturb binding significantly (Glu30, Leu33, Val34, Val37, Glu41, Gly49, Ser50, Asp51, Tyr54, Tyr55, Pro56, and Val68). With one exception (Val68), all these residues come from helices II and III and lie clustered together in Im9 (colored red, magenta, and yellow in Figure 5b,e). All of the remaining 22 residues

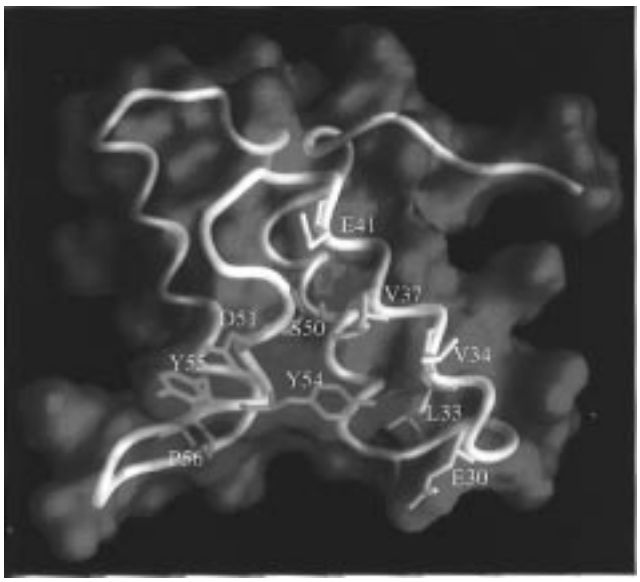

FIGURE 6: Structure of Im9 showing the residues which dominate the binding interactions toward the E9 DNase. The ten residues which the alanine scan data suggest are the major contributors toward E9 DNase binding energy are shown in the figure. Color code: red, residues from helix III which act as the anchor of the E9 DNase binding site; green, variable residues of helix II which govern protein−protein interaction specificity.

(two-thirds of those mutated) fall below the fitted line; 11 show $\Delta\Delta G_{binding}$ of <0.5 kcal/mol (labeled blue in Figure 5b) and 11 of 0.5−1 kcal/mol (labeled green in Figure 5b). Many of these residues flank the energetically important amino acids.

In agreement then with the NMR data, the alanine scan suggests that the major binding interactions are centered around residues on helix II and helix III (Figure 5). In addition, it seems that many of the residues on the underside of the two helices are not important for binding (compare Figure 5d with Figure 5e). While there is general agreement between the NMR and mutagenesis data, there are some notable discrepancies. Several residues which showed substantial chemical shift perturbations in the NMR experiments (such as Lys35 and Ser28) have no effect on E9 DNase binding when substituted for alanine while other residues, such as Asp51, fell below the cutoffs used in interpreting the chemical shift changes observed in the HSQC experiments but make substantial interactions toward the E9 DNase. Notwithstanding these caveats, it is clear that the NMR experiments provided a good working model of the E9 DNase binding surface of Im9, which has been substantiated by the alanine scan.

Further analysis of the 12 residues identified in Figure 4B suggests that they may not all be directly involved in binding. $\Delta\Delta G_{binding}$ due to the Gly49Ala mutation is almost certainly due to disruption of steric complementarity at the complex interface since it results in the addition of a side chain rather than its removal. The side chain of Val68 is buried between helices I and IV in the Im9 structure and is the only residue highlighted by this analysis which is not part of the helix II/helix III interface. Its effect on $\Delta\Delta G_{binding}$ may be due to changes in protein conformation rather than direct participation in binding, and this would be compatible with the large $\Delta\Delta G_{stability}$ (Figure 4). The same could apply to other buried residues such as Val37, which disrupts binding and stability to a similar extent as Val68.

Leu33 and Tyr54 are two residues which have substantial effects on both binding and stability (Figure 4B). Their effects on binding, however, are unlikely to be solely through changes in stability since other (buried) residues near the binding site are even more destabilizing but have a minimal effect on binding (for example, His46 and Ile53). A significant portion of Tyr54 is exposed to solvent, forming part of a hydrophobic patch on the surface of Im9 bridging Tyr55 and Val34, both important binding residues. Hydrophobicity is an important component of protein−protein interactions (*26*−*28*), and so it seems likely that Tyr54 serves both a structural and functional role in Im9. Similar arguments apply to Leu33, although unlike Tyr54 a significant portion of the side chain of this residue is buried in the hydrophobic core of Im9. Even so, $\Delta\Delta G_{binding}$ on substitution for alanine is much greater than that seen for other residues of similar accessibility and stability, for example, Leu36 and Val37 (Figure 4A), implying a role in binding.

In summary, the alanine mutagenesis data point to 10 residues (Glu30, Leu33, Val34, Val37, Glu41, Ser50, Asp51, Tyr54, Tyr55, and Pro56) as being important for binding the E9 DNase, all of which project from helices II and III. Seven of these have little effect on the stability of Im9 when substituted for alanine (Glu30, Val34, Glu41, Ser50, Asp51, Tyr55, and Pro56), while the remaining three residues (Leu33, Val37, and Tyr54) appear to have both structural and functional roles.

DISCUSSION

Problems in Protein−Protein Recognition. In recent years a number of systems have provided important information on the structures and thermodynamics of protein complexes. Examples include hormone−receptor complexes (*20*, *27*, *29*), RNase−inhibitor complexes (*21*, *30*, *31*) and antibody−antigen complexes (*32*−*35*). Nevertheless, two key questions concerning protein−protein recognition remain to be answered. (1) Why do different protein complexes possess different affinities? (2) How is specificity defined in families of homologous proteins? The first question, related to the biological role of the complex, highlights one of the main problems in protein−protein recognition, that of the very diverse affinities that can describe interprotein complexes; for example, the K_ds for the complexes cited above range from 10^{-6} to 10^{-14} M. Calculating protein complex binding affinities has proven elusive (*36*) although there have been successful empirical models (*32*) based primarily on the amount of buried surface area in protein−protein complexes (*37*, *38*). The second question arises because within a family of homologous proteins binding specificity must be built upon a common structural framework. In antigen−antibody complexes, for example, K_ds ranging from 10^{-6} to 10^{-9} M are achieved by six variable loops built upon the conserved β-sheet framework structure of the immunglobulin fold (*34*, *35*). While the sequence of the loops is undoubtedly the main determinant of antibody specificity, the framework itself can affect the conformation of the loops and hence specificity (*39*). The DNase-specific immunity proteins Im2, Im7, Im8, and Im9 bind the E9 DNase with dissociation constants ranging from 10^{-4} to 10^{-16} M (*14*). Therefore, this is a

unique system in which to address how such varied stabilities can be achieved within a family of structurally homologous proteins.

A Dual Recognition Model for Immunity Specificity. We have proposed previously that the differing stabilities of cognate versus noncognate interactions could be determined by a few key residues whose contribution to binding energy is dependent on their structural context (*14*). The results of the alanine scan provide experimental evidence for such a mechanism of selectivity. The main DNase binding interactions on Im9 are dominated by up to 10 residues: five from helix III (Ser50, Asp51, Tyr54, Tyr55, and Pro56) and five from helix II (Glu30, Leu33, Val34, Val37, and Glu41).

The residues from helix III make the largest relative contribution to DNase binding, accounting for approximately two-thirds of the binding energy (whether amino acids which affect protein stability are included or not). Importantly, these residues are conserved in the immunity protein family (Figure 5c). The residues displayed from helix II are not conserved and while only contributing around one-third of the relative binding energy are known to govern colicin−DNase binding specificity (*15*). This is analogous to other protein complexes where residues which govern specificity do not themselves contribute significantly to the binding energy (*40, 41*). Our data argue for a *dual recognition* model for colicin−immunity binding in which the conserved residues of helix III serve as the anchor of the binding site and contribute the greatest binding energy while the variable residues of helix II make a relatively small contribution to binding energy but determine the specificity of the protein−protein interaction.

The apparent binding energy associated with the five conserved anchor residues of helix III in the cognate Im9−E9 DNase interaction is of the order of 15−19 kcal/mol. Yet the E9 DNase binding energy associated with the noncognate immunity proteins Im7, Im8, and Im2 is ∼6, 8, and 10 kcal/mol, respectively (*14*). Since the structures of the immunity proteins are very similar (*11, 12*), this implies that these residues cannot contribute the same binding energy in the noncognate complexes. In other words, the potentially stabilizing interactions of the anchor residues of helix III are modulated by the specificity-determining residues of helix II. This model further implies that the residues of helix II serve two roles: making unique interactions that contribute to binding energy (approximately one-third in a cognate complex) and participating in steric and electrostatic clashes which modulate the stabilizing interactions emanating from the conserved residues of helix III.

Modulation of Anchor Interactions by the Specificity-Determining Residues of Helix II. Closer inspection of the residues on the surface of helix II suggests ways in which this modulation might occur, for example, position 34 which abuts the binding site anchor of helix III (Figure 5a,b). In the cognate E9 DNase−Im9 complex Val34 makes a significant interaction with the E9 DNase since mutating it to alanine destabilizes binding by 2.6 kcal/mol but does not affect the stability of Im9 itself (Figure 4). Furthermore, it seems likely that a hydrophobic recognition site on the E9 DNase exists that is designed to accept the valine side chain of position 34 in Im9. This being the case, it is of interest to note that the magnitude of complex destabilization that results from the Val34Ala substitution is of the same order as that expected for the removal of buried methyl groups from the hydrophobic core of a folded protein (*42*); in several mutagenesis studies it has been found that the conformational stability of a protein is destabilized by 1.5 ± 0.5 kcal/mol per buried methylene. This is similar to the destabilization energy associated with the removal of each of the methyl groups of Val34 in the E9 DNase−Im9 complex (1.3 kcal/mol), implying that this residue fits into a closely packed, hydrophobic pocket on the surface of its target enzyme. The relevance of this comparison to specificity in the colicin DNase−immunity system becomes clear from the identity of this residue in other immunity proteins; position 34 is an aspartic acid residue in Im8 and Im7 and an asparagine residue in Im2. Indeed, substituting the valine of Im9 for an aspartic acid residue found in Im8 causes the resulting mutant protein to cross-react with colicin E8 in a biological plate assay even though Im9 itself does not show such cross-reactivity (*43*).

The presence of an unpaired charge in the hydrophobic core of a globular protein is highly destabilizing (*42*). Placed in the context of the alanine scanning data on Im9 and the specificity differences between the immunity proteins, part of the mechanism of specificity for these proteins may have its basis in this fundamental principle of protein stability. Assuming that all the immunity proteins have the capacity to form the stabilizing anchor interactions (from helix III), then achieving these with a noncognate immunity protein might result in the immersion of a charged or polar residue in a binding pocket on the E9 DNase designed to accommodate a hydrophobic residue. In this way, the stabilizing interactions of the binding site anchor could be counteracted by the instability generated from having the wrong amino acid at position 34. Similar situations could pertain for other residues along helix II such as position 41 which is a glutamic acid in Im9 (and contributes ∼2 kcal/mol binding energy) but an isoleucine and leucine residue in Im8 and Im7, respectively.

Colicin−Immunity Protein Complexes and Other Protein−Protein Interaction Systems. The analogy between protein−protein recognition and the topology of a folded protein has previously been recognized by others, a good example being the work of Wells and co-workers on growth hormone binding to its receptor (*27, 41*). An alanine scan across the binding surfaces of both binding partners showed that the main determinants of complex stability were complementary hydrophobic interactions at the center of the binding site while peripheral residues tended to be polar or charged groups that contributed little to binding energy but which were implicated in receptor specificity. There are some similarities to the E9 DNase−Im9 interaction since some of the main binding determinants in Im9 are large hydrophobic groups (two tyrosines and a valine). There are significant differences however, such as the presence of an important charged residue, Asp51, in the binding site and the involvement of hydrophobic residues such as Val34 in specificity. Several polar and charged residues have already been identified in the E9 DNase as being involved both in specificity (*44*) and in the mechanism of the enzyme (*17*), and these residues may be involved in the interaction with the charged groups of Im9.

The modulation of binding energy from conserved interaction sites by neighboring variable residues would appear to

be a mechanism of specificity that is operating in other protein families as well as colicin−immunity complexes. Signal transduction proteins, for example, which contain conserved SH2 and SH3 domains all recognize a specific motif, phosphotyrosyl-containing peptides and polyproline sequences, respectively, but specificity is mediated through neighboring nonconserved residues (*45*, *46*). Interestingly, this mediation can take the form of charged-for-hydrophobic residue substitutions as in the case of the Fyn tyrosine kinase SH3 domain binding the HIV-1 Nef protein with high affinity (*46*, *47*).

Modulation of binding energy by destabilizing interactions has also been used to select specific topological isomers of four helical bundles in the area of protein design (*48*). Although this destabilization was primarily through repulsion of like charges, it may be possible to engineer similar topological restraints by charge-for-hydrophobic residue substitutions as occurs in the immunty protein system.

In conclusion, our observation that conserved residues dominate the binding interaction between immunity proteins and colicin DNases may be a general phenomenon in protein−protein recognition involving structurally homologous proteins. This is a logical mechanism of selectivity in evolutionary terms since the appearance of novel specificities need only require the mutation of a select few residues which modulate the binding interactions emanating from the conserved protein scaffold.

ACKNOWLEDGMENT

We thank Ann Reilly for expert technical assistance and Dr. Andrew Hemmings for helpful discussions. We also thank the reviewers of this paper for their perceptive comments, especially with regard to the presentation of the data in Figure 4.

REFERENCES

1. James, R., Kleanthous, C., and Moore, G. R. (1996) *Microbiology 142*, 1569−1580.
2. Ohno-Iwashita, Y., and Imahori, K. (1980) *Biochemistry 19*, 652−659.
3. Wallis, R., Reilly, A., Barnes, K., Abell, C., Campbell, D. G., Moore, G. R., James, R., and Kleanthous, C. (1994) *Eur. J. Biochem. 220*, 447−454.
4. Lau, C. K., Parsons, M., and Uchimura, T. (1992) in *Bacteriocins, microcins and lantibiotics* (James, R., Lazdunski, C., and Pattus, F., Eds) pp 353−378, NATO ASI Series H, Springer, Heidelberg.
5. Jakes, K. S., and Zinder, N. D. (1974) *Proc. Natl. Acad. Sci. U.S.A. 71*, 3380−3384.
6. Schaller, K., and Nomura, M. (1976) *Proc. Natl. Acad. Sci. U.S.A. 73*, 3989−3993.
7. Wallis, R., Reilly, A., Rowe, A., Moore, G. R., James, R., and Kleanthous, C. (1992) *Eur. J. Biochem. 207*, 687−695.
8. Pugsley, A. P., and Schwartz, M. (1983) *Mol. Gen. Genet. 190*, 366−372.
9. Pugsley, A. P. (1984) *Microbiol. Sci. 1*, 203−205.
10. Osborne, M. J., Lian, L.-Y., Wallis, R., Reilly, A., James, R., Kleanthous, C., and Moore, G. R. (1994) *Biochemistry 33*, 12347−12355.
11. Osborne, M. J., Breeze, A., Lian, L.-Y., Reilly, A., James, R., Kleanthous, C., and Moore, G. R. (1996) *Biochemistry 35*, 9505−9512.
12. Chak, K.-F., Safo, M. K., Ku, W.-Y., Hsieh, S.-Y., and Yuan, H. S. (1996) *Proc. Natl. Acad. Sci. U.S.A. 93*, 6437−6442.
13. Wallis, R., Moore, G. R., James, R., and Kleanthous, C. (1995) *Biochemistry 34*, 13743−13750.
14. Wallis, R., Leung, K.-Y., Pommer, A. J., Videler, H., Moore, G. R., James, R., and Kleanthous, C. (1995) *Biochemistry 34*, 13751−13759.
15. Li, W., Dennis, C. A., Moore, G. R., James, R., and Kleanthous, C. (1997) *J. Biol. Chem. 272*, 22253−22258.
16. Osborne, M. J., Wallis, R., Leung, K.-Y., Williams, G., Lian, L.-Y., Kleanthous, C., and Moore, G. R. (1997) *Biochem. J. 323*, 823−831.
17. Garinot-Schneider, C., Pommer, A. J., Moore, G. R., Kleanthous, C., and James, R. (1996) *J. Mol. Biol. 260*, 731−742.
18. Kellis, J. T., Jr., Nyberg, K., Sali, D., and Fersht, A. R. (1988) *Nature 333*, 784−786.
19. Shrake, A., and Rupley, J. A. (1973) *J. Mol. Biol. 179*, 351−371.
20. Cunningham, B. C., and Wells, J. A. (1993) *J. Mol. Biol. 234*, 554−563.
21. Schreiber, G., and Fersht, A. R. (1993) *Biochemistry 32*, 5145−5150.
22. Janin, J. (1995) *Biochimie 77*, 497−505.
23. Pace, C. N. (1975) *CRC Crit. Rev. Biochem. 3*, 1−43.
24. Spitzfaden, C., Weber, H.-P., Braun, W., Kallen, J., Wider, G., Widmer, H., Walkinshaw, M. D., and Wüthrich, K. (1992) *FEBS Lett. 300*, 291−300.
25. Benjamin, D. C., Williams, D. C., Jr., Smith-Gill, S. J., and Rule, G. S. (1992) *Biochemistry 31*, 9539−9545.
26. Young, L., Jernigan, R. L., and Covell, D. G. (1994) *Protein Sci. 3*, 717−729.
27. Clackson, T., and Wells, J. A. (1995) *Science 267*, 383−386.
28. Jones, S., and Thornton, J. M. (1996) *Proc. Natl. Acad. Sci. U.S.A. 93*, 13−20.
29. De Vos, A. M., Ultsch, M., and Kossiakof, A. A. (1992) *Science 255*, 306−312.
30. Schreiber, G., and Fersht, A. R. (1995) *J. Mol. Biol. 248*, 478−486.
31. Guillet, V., Lapthorn, A., Hartley, R. W., and Maugue, Y. (1993) *Structure 1*, 165−176.
32. Novotny, J., Bruccoleri, R. E., and Saul, F. A. (1989) *Biochemistry 28*, 4735−4749.
33. Hawkins, R. E., Russell, S. J., Baier, M., and Winter, G. (1993) *J. Mol. Biol. 234*, 958−964.
34. Wilson, I. A., and Stanfield, R. L. (1993) *Curr. Opin. Struct. Biol. 3*, 113−118.
35. Davies, D. R., and Cohen, G. H. (1996) *Proc. Natl. Acad. Sci. U.S.A. 93*, 7−12.
36. Janin, J. (1995) *Proteins 21*, 30−39.
37. Horton, N., and Lewis, M (1992) *Protein Sci. 1*, 169−181.
38. Covell, D. G., and Wallqvist, A. (1997) *J. Mol. Biol. 269*, 281−297.
39. Foote, J., and Winter, G. (1992) *J. Mol. Biol. 224*, 487−499.
40. Cunningham, B. C., and Wells, J. A. (1991) *Proc. Natl. Acad. Sci. U.S.A. 88*, 3407−3411.
41. Wells, J. A. (1996) *Proc. Natl. Acad. Sci. U.S.A. 93*, 1−6.
42. Fersht, A. R., and Serrano, L (1993) *Curr. Opin. Struct. Biol. 3*, 75−83.
43. Wallis, R., Moore, G. R., Kleanthous, C., and James, R. (1992) *Eur. J. Biochem. 210*, 923−930.
44. Curtis, M. D., and James, R. (1991) *Mol. Microbiol. 5*, 2727−2733.
45. Feller, S. M., Ren, R., Hanafusa, H., and Baltimore, D. (1994) *Trends Biochem. Sci. 19*, 453−458.
46. Lee, C.-H., Saksela, K., Mirza, U. A., Chait, B. T., and Kuriyan, J. (1996) *Cell 85*, 931−942.
47. Lee, C.-H., Leung, B., Lemmon, M. A., Zheng, J., Cowburn, D., Kuriyan, J., and Saksela, K. (1995) *EMBO J. 14*, 5006−5051.
48. Betz, S. F., Liebman, P. A., and DeGrado, W. F. (1997) *Biochemistry 36*, 2450−2458.

BI971884A